scientific reports

Check for updates

OPEN

Thermal performance of Falkner Skan model (FSM) for ($GOMoS_2$)/($C_2H_6O_2$-H_2O) 50:50% nanofluid under radiation heating source

Mutasem Z. Bani-Fwaz[1], Adnan[2], Sami Ullah Khan[3], B. Shankar Goud[4], Tadesse Walelign[5]✉, Kanayo Kenneth Asogwa[6] & Iskander Tlili[7]

The hybrid base solvent water (H_2O) and ethylene glycol ($C_2H_6O_2$) are highly use in industrial applications due to excellent solvability. Addition of hybrid nanoparticles (GO-MoS_2) augments the thermal conductivity of these fluids which ultimately make them very productive. Hence, the current study aims to develop and investigate the novel hybrid nanofluid model (GO-MoS_2)/($C_2H_6O_2$-H_2O) through MRW (moving riga wedge) and SRW (static riga wedge) cases. The traditional Falkner Skan Model (FSM) is modified using the novel effects of solar radiations, internal heating source and fixed magnets which is associated to the concept of Riga wedge. Further, the improved thermal-physical characteristics of hybrid nanofluids will use to enhance the thermal productivity. A mathematical model is developed for the flow situation of (GO-MoS_2)/($C_2H_6O_2$-H_2O) and treated numerically. The results furnished through graphical way and comprehensive discussion provided. It is examined that the movement of (GO-MoS_2)/($C_2H_6O_2$-H_2O) reduced for MRW and observed the rapid velocity near the surface. The heat generating source and solar radiations number enhanced the performance of (GO-MoS_2)/($C_2H_6O_2$-H_2O) and better predicted ranges for these parameters are observed from $Q = 0.1, 0.2, 0.3, 0.4$ and $Rd = 1.0, 2.0, 3.0, 4.0$. Moreover, the boundary layer region becomes thin for heating source and it increased for stronger solar radiation effects. The nanoparticle amount of GO and MoS_2 enhanced the model utilization while higher magnetic number and MRW number λ controlled the thermal boundary layer. The results for the model dynamics are noticed dominant for MRW case as compared to SRW case.

Keywords Hybrid nanofluid, Nanoparticles, Solar radiations, Falkner Skan flow, Heating source

Heat transport phenomena in fluids are a significant research motive in numerous engineering systems and industries. These include, but are not limited to, heating and cooling of buildings, chemical engineering, applied and mechanical engineering, etc. Although conventional fluids (water, EG, kerosene oil, etc.) have excellent solvability characteristics but low thermal conductivity, due to which these fluids have a weak heat transfer rate. Therefore, the heat transfer performance of common fluids can be enhanced by dispersing nanometer-sized particles. The resultant fluid, commonly known as nanofluid, has better heat transfer possibilities than common fluids. Researchers from different fields put their efforts into the formulation of efficient nanofluid models from different physical aspects.

Nanofluid is simply a uniform mixture of one type of nanoparticle and the base fluid. In 2021, Madhukesh et al.[1] conducted a comprehensive study on hybrid nanofluid by considering AA7072 and AA7075 alloys. The authors formulated the problem of stretching surfaces under the innovative effects of resistive heating and non-fourier heat flux. The outcomes revealed that aluminum alloys-based hybrid nanofluids have good heat transfer rate than water. Animasaun et al.[2] were inspired by the joint thermal conductivity of ternary nanoparticles and

[1]Department of Chemistry, College of Science, King Khalid University, P. O. Box 9004, Abha 61413, Saudi Arabia. [2]Department of Mathematics, Mohi-ud-Din Islamic University, Nerian Sharif, Trarkhel 12080, Pakistan. [3]Department of Mathematics, Namal University, Mianwali 42250, Pakistan. [4]Department of Mathematics, JNTUH University College of Engineering, Science and Technology, Hyderabad 500085, Telangana, India. [5]Department of Mathematics, Debre Tabor University, Debre Tabor, Ethiopia. [6]Department of Mathematics, Nigeria Maritime University, Okerenkoko, Delta State, Nigeria. [7]Department of Mechanical Engineering, Faculty of Engineering, Islamic University of Madinah, Madinah 42351, Saudi Arabia. ✉email: tadelenyosy@gmail.com

investigated the effects of an unsteady parameter on the model dynamics through a convective surface. They observed that when the surface angle approaches to 90^o, the unsteady acceleration decreases while convective acceleration enhances. The thermal radiative aspects of Casson nanofluid in the presence of internal heat absorption/generation sources have been discussed by Saeed et al.[3]. It was concluded that the energy transport enhanced with an increase in the thermal radiative source and the boundary layer thickness decreased for larger values of the rotating parameter.

The static or moving wedge conditions extensively alter the motion and thermal behaviour of the fluids. Hence, Mahanthesh et al.[4] extended the work for moving case for heat transfer enhancement. The authors considered ZnO-EG as working fluid and performed sensitivity analysis if the model. The significant effects of wedge movement are examined on the velocity and heat transport rate. Another study regarding the Falkner Skan flow under the impacts of freezing temperature and molecular diameter effects were examine in[5]. Vahedi et al.[6] focused on the characteristics of wedge flow for electrically conducted Cu/water. They found that the thermal and hydrodynamic boundary layers depreciated for stronger magnetic number and smaller wedge angle. Among the nanomaterials, ferromagnetic material has their own significance due to their structure and magnetic properties. Therefore, Gowda et al.[7] explored the impacts of magnetic dipoles on the functionality of nanofluid comprising ferromagnetic nanoparticles. Further, the effects of Stefan heating also included in the model and handled the nanofluid model numerically. It was concluded that convective thermal condition has tendency to enhance the heat transfer rate in nanofluid.

Use of MHD, heating source and radiations are of larger interest in various disciplines particularly in thermal engineering. Implications of these phenomenon contribute effectively in transport mechanism of hybrid nanofluids. Kumar et al.[8] used radiations effects for thermal applications of hybrid nanofluids. The analysis carried for radiated wedge and examined thermal enhancement due to strengthening the radiation source. The obtained data compared with previous once and validated the study. Sajjan et al.[9] and Raju et al.[10] extended the concept of nonlinear radiations, nanomaterials shape, and Darcy effects for boundary layer and permeable channel, respectively. The hybrid nanofluids are taken under the effects of shapes and varying thermal conductivities. They found that role of nonlinear radiations is crucial for thermal applications while Darcy phenomena opposes the hybrid nanofluid motion. The study of quadratic and linear convection on the transport mechanism of multiple nanoparticles based model have been discussed in[11]. The efficiency of hybrid nanofluid is observed high than that conventional nanofluids and suggested that modified nanofluids are reliable for thermal applications.

Recently, Goud et al.[12] and Mahmood et al.[13] reported the numerical analysis of Newtonian and non-Newtonian nanofluid models under varying physical conditions. The results validated with open literature and examined that (Al_2O_3-Cu)/H_2O hybrid nanofluid has excellent thermal characteristics. Insertion of unsteady effects in the nanofluid modelling highly affect the model performance. Keeping in mind the significance of unsteady phenomena, Alghamdi et al.[14], Fwaz et al.[15], Khadija et al.[16] and Adnan et al.[17] investigated different nanoliquid problems for heat transfer applications. The authors accommodated important physical phenomena and found excellent outcomes for nanofluids. They recommended that nanofluids have better momentum and heat transfer abilities which are important form industrial applications. The CNTs termed as carbon nanotubes obtained much interest of the researchers in the last few decades. This is heat transfer nanomaterial having fascinating structure. Different studies (see Refs[18–21]). on the performance of CNTs based fluid dynamics models have been discussed by various experts in the field and agreed that the CNTs have excellent heat transmission ability under laminar flow regimes.

Reddy et al.[22] investigated hydromagnetic based (Ag-CuO)/H_2O model and performed sensitivity analysis under thermal radiation impacts. The problem is associated to the convective surface and found that the efficiency of hybrid nanofluid enhanced as the convection effects increases. Shamshuddin et al.[23,24] and [25], provided deep analysis of nanofluids and checked the thermal progress through different methodologies. Impacts of ferromagnetic, MHD and resistive heating are observed. The studies explored that nanofluids are innovative class which have considerable thermal efficiency compared to simple fluids.

The study of hybrid and ternary nanofluids for heat transfer applications cannot be ignored because these fluids providing an excellent enhanced properties like thermal conductivity, heat capacity, electrical conductivity and dynamic viscosity etc. In recent years, researchers turned towards thermal investigation in advanced nanofluids by engaging variety of nanomaterials. A study for hybrid nanofluid under solar thermal radiative effects has been reported by Waqas et al.[26] and Ferdows et al.[27] performed numerical simulation for heat and mass transport in nanofluids using single and two phase models. The authors used Al_2O_3, Cu and GO nanoparticles[28] to enhance the characteristics of conventional fluids. The studies revealed that velocity enhanced with increasing Deborah effects while higher Schmidt number values encouraged the mass transfer. Further, the authors suggested that hybrid nanoliquids have enhanced heat and mass transport rate and recommended better for practical applications. Further, comprehensive literature and key findings of the studies are given in Table 1.

In the view of above reported studies, it is noticed that although numerous attempts have been made for the thermal analysis in common, nano and hybrid nanofluids through wedge under different physical circumstances. However, there are still some openings for mathematical modelling and analysis of heat transfer for advanced nanoliquids through Riga wedge. The novelty of the hybrid nanofluid problem will enhance by including the influences of fixed magnets due to Riga case, solar radiations, nanoparticle's concentrations and internal heating species. Thus, the key objectives of the research are:

- To introduce the concept of Riga wedge and how it alter the flow dynamics and heat transfer rate.
- To develop the heat transfer problem for hybrid nanofluid using effective characteristics with special emphasize on moving and static wedge cases.
- To investigate the influences of solar radiations and internal heating source on the overall performance of the model.

Authors	Type of fluid and flow	Physical effects	Core findings
Alqahtani et al.[29]	Newtonian, laminar and steady	Magnetic field, Soret and Schmidt effects	Mass transfer enhanced for stronger Schmidt number values
Kudenatti and Jyoth[30]	2D boundary layer flow of Newtonian fluid	Prandtl and viscous dissipation effects	Boundary layer thickness observed thinner for increasing pressure gradient
Amar et al.[31]	Steady flow	MHD, thermal convection and heating source	The heat transfer rate augmented for heating generation, reduced for heat absorption, and the temperature enhanced for Eckert number values
Anuar et al.[32]	Hybrid nanofluid	Modified boundary conditions and permeability impacts	Boundary layer separation is observed minimum for large nanoparticles amount and hybrid nanofluid declared more effective than simple nanofluid
Zeeshan et al.[33]	Mono nanofluid	MHD, thermophoresis and Brownian movement effects	The model sensitivity performed using RSM and examined that the Nt and Nb are more sensitive parameters of the model

Table 1. Literature review for boundary layer flows under different physical circumstances.

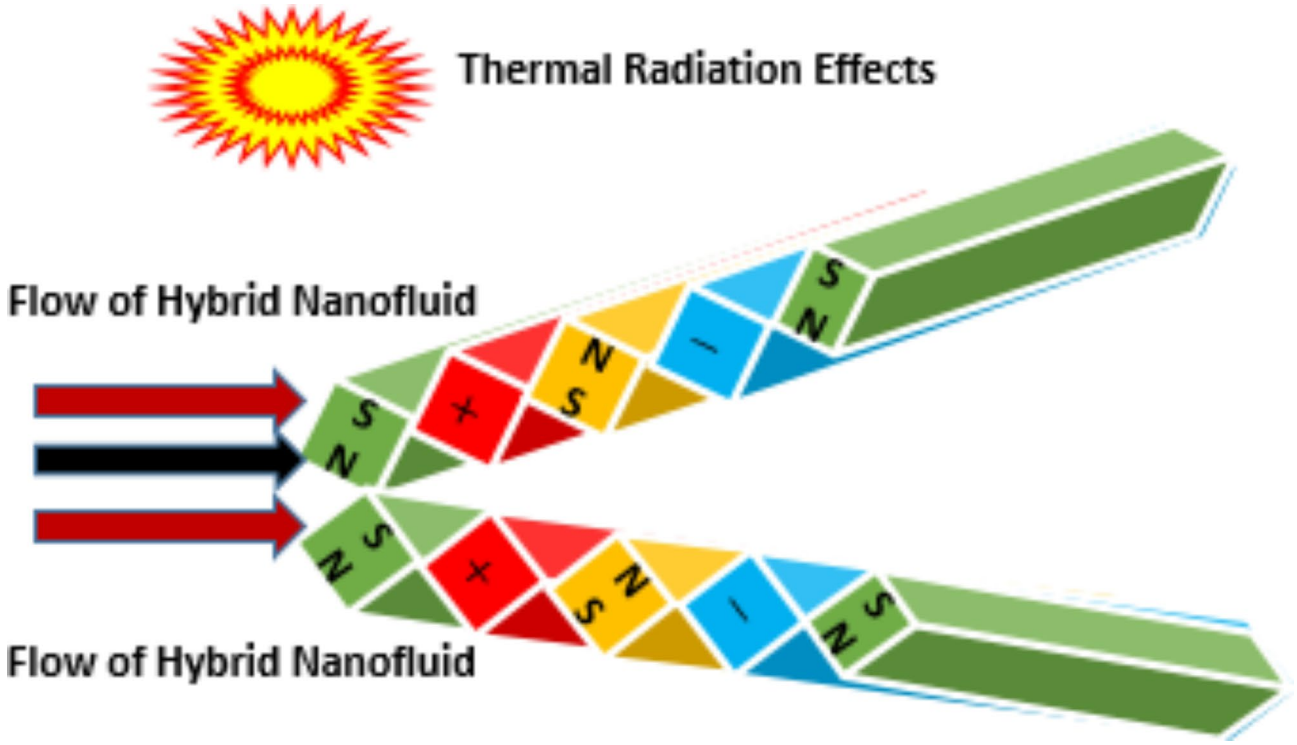

Fig. 1. The hybrid nanofluid (GO-MoS_2)/($C_2H_6O_2$-H_2O) components.

- To estimate the comparative results for fluid movement and thermal transport through static and moving wedges.

Model development

In this study, consider Falkner Skan flow (FSF) of ternary nanofluid under steady state condition. To enhance the functionality of water, the hybrid nanoparticles (Go-MoS_2) are used with uniform dispersion characteristics. The base liquid is taken as water due to excellent solvability. The coordinates are designated in such a way that the x-component is in the direction of wedge. The wedge surface is made by alternating arrangements of magnets due to which is called Riga wedge. The temperature near the working surface and at ambient locations are taken as T_w and T_∞, respectively. Further, the accelerating wedge and free stream velocities are $u_w = x^m U_w$ and $u_e = x^m U_\infty$ ($0.0 \leq m \leq 1$ and U_w, U_∞). The hybrid nanofluid components are demonstrated in Fig. 1. Further restrictions for the model formulation are as under:

- The functional ternary fluid possesses incompressibitly characteristics and there is no chemical species present therein.
- The hybrid nanoparticles (Go-MoS_2) and primary solvent are thermally in equilibrium.

The primary physical laws which possesses the BLF of ternary nanoliquid through a Riga wedge are described in the subsequent mathematical expressions[34,35].

$$u_x + v_y = 0 \tag{1}$$

$$u_x u + u_y v = u_e u_e' + \frac{\mu_{\,hybridnano}}{\rho_{\,hybridnano}} u_{yy} + \frac{M_o J_o \pi}{8\rho_{\,hybridnano}} e^{(-\frac{\pi}{a} y)} \tag{2}$$

$$T_x u + T_y v = \frac{k_{hybridnano}}{(\rho\, c_p)_{hybridnano}} T_{yy} + \frac{16\sigma^{\,*} T_\infty^3}{3k^*(\rho\, c_p)_{hybridnano}} T_{yy} + \frac{Q}{(\rho\, c_p)_{hybridnano}} (T_w - T_\infty) \tag{3}$$

The fluid flow is subject to the subsequent conditions at the RWS (Riga wedge surface) and at free stream positions. Further the similarity transformative functions for the present investigation are described in Eq. (5). The term χ represents the stream function and the velocity components are obtained using $u = \chi_{\,y}$ and $v = -\chi_{\,x}$ which satisfy the law of conservation of mass.

$$u = u_w\downarrow_{\,y=0},\ T = T_w\downarrow_{\,y=0},\ v = 0,\ u \to\ u_e\downarrow_{\,y\to\infty},\ T \to\ T_\infty\downarrow_{\,y\to\infty} \tag{4}$$

$$\eta\ = \left(\frac{u_e\,(x)\,(m+1)}{2x\nu_{\,f}}\right)^{0.5} y,\ \beta\ (\eta) = \frac{T - T_\infty}{T_w - T_\infty},\ \chi\ = \left(\frac{2xu_e\,(x)\,\nu_{\,f}}{m+1}\right)^{0.5} F(\eta) \tag{5}$$

The formulas for significant factors for the present ternary nanofluid model are given in Eqs. (6, 7), respectively.

$$C_{skinfric} = \frac{\mu_{\,hybridnano}}{u_e^2 \rho_{\,f}} u_y\downarrow_{\,y=0} \tag{6}$$

$$Nu = -x\left[\frac{k_{hybridnano} + q_y}{k_f\,(T_w - T_\infty)}\right] T_y\downarrow_{\,y=0} \tag{7}$$

Further, the effective formulas for ternary nanofluid properties like electrical conductivity, thermal conductivity, heat capacity and dynamic viscosity are expressed in Table 2 (see Refs[36–38]). where, $\widehat{\mathfrak{H}}_2 = \varphi_{\,2}$and $\widehat{\mathfrak{H}}_1 = \varphi_{\,1}$ are the nanoparticles concentrations. Moreover, the values of nanoparticles and their response on the ternary nanofluid characteristics[39] are furnished in Figs. 2 and 3, respectively.

Now, by practicing the similarity rules and the characteristics of hybrid nanofluids, the following nonlinear mathematical model is obtained which possesses the laminar steady flow through a Riga wedge under solar radiations and heating source effects. Further, the reduced form of the flow conditions are given in Eq. (10).

$$\frac{\frac{\mu_{\,hybridnano}}{\mu_{\,pf}}}{\frac{\rho_{\,hybridnano}}{\rho_{\,pf}}} F''' + FF'' + \frac{2m}{1+m}\left[1 - F'^{\,2}\right] + \frac{\sigma_{\,hybridnano}}{\sigma_{\,pf}} Me^{-\alpha\,\eta} = 0 \tag{8}$$

$$\left(\frac{k_{hybridnano}}{k_{pf}} + \frac{4}{3}Rd\right)\beta'' + \frac{\Pr(\rho\, c_p)_{hybridnano}}{(\rho\, c_p)_{pf}}\left[F\beta' + Q\beta\right] = 0 \tag{9}$$

$$F(0) = 0,\ F'\ (0) = \lambda,\ F'\ (\infty) = 1,\ \beta\ (0) = 1,\ \beta\ (\infty) = 0 \tag{10}$$

Ternary Nanofluids Property	Representation	Properties Formulas
Heat Capacity	$\frac{(\rho\, c_p)_{hybridnano}}{(\rho\, c_p)_{pf}}$	$\left[\left(1-\widehat{\mathfrak{H}}_2\right)\left(1-\widehat{\mathfrak{H}}_1+\frac{\widehat{\mathfrak{H}}_1(\rho\, c_p)_{Go}}{(\rho\, c_p)_{pf}}\right)+\frac{\widehat{\mathfrak{H}}_2(\rho\, c_p)_{MoS_2}}{(\rho\, c_p)_{pf}}\right]$
Density	$\frac{\rho_{\,hybridnano}}{\rho_{\,pf}}$	$\left[\left(1-\widehat{\mathfrak{H}}_2\right)\left[\left(1-\widehat{\mathfrak{H}}_1+\frac{\widehat{\mathfrak{H}}_1\rho_{\,Go}}{\rho_{\,pf}}\right)\right]+\frac{\mathfrak{H}_2\rho_{\,MoS_2}}{\rho_{\,pf}}\right]$
Dynamic Viscosity	$\frac{\mu_{\,hybridnano}}{\mu_{\,pf}}$	$\frac{1}{\left(1-\widehat{\mathfrak{H}}_1\right)^{2.5}\left(1-\widehat{\mathfrak{H}}_2\right)^{2.5}}$
Thermal Conductivity	$\frac{k_{hybridnano}}{k_{pf}}$	$\frac{k_{(Go-MoS_2)}}{(k_{Gopf})} = \left[\frac{\breve{k}_{MoS_2}+2\breve{k}_{(Go)_{pf}}-2\widehat{\mathfrak{H}}_2\left(\breve{k}_{(Go)_{pf}}-\breve{k}_{MoS_2}\right)}{\breve{k}_{MoS_2}+2\breve{k}_{(Go)_{pf}}+\widehat{\mathfrak{H}}_2\left(\breve{k}_{(Go)_{pf}}-\breve{k}_{MoS_2}\right)}\right]$ $\breve{k}_{(Go)_{pf}} = k_{pf}\left[\frac{\breve{k}_{Go}+2\breve{k}_{pf}-2\widehat{\mathfrak{H}}_1\left(\breve{k}_{pf}-\breve{k}_{Go}\right)}{\breve{k}_{Go}+2\breve{k}_{pf}+\widehat{\mathfrak{H}}_1\left(\breve{k}_{pf}-\breve{k}_{Go}\right)}\right]$
Electrical Conductivity	$\frac{\sigma_{\,hybridnano}}{\sigma_{\,pf}}$	$\frac{\sigma_{\,(Go-MoS_2)_{pf}}}{\sigma_{\,(Go)_{pf}}} = \frac{\sigma_{\,MoS_2}+2\sigma_{\,(Go)_{pf}}-2\widehat{\mathfrak{H}}_2\left(\sigma_{\,(Go)_{pf}}-\sigma_{\,MoS_2}\right)}{\sigma_{\,MoS_2}+2\sigma_{\,(Go)_{pf}}+\widehat{\mathfrak{H}}_2\left(\sigma_{\,(Go)_{pf}}-\sigma_{\,MoS_2}\right)}$ $\frac{\sigma_{\,(Go)_{pf}}}{\sigma_{\,pf}} = \frac{\sigma_{\,Go}+2\sigma_{\,pf}-2\widehat{\mathfrak{H}}_1\left(\sigma_{\,pf}-\sigma_{\,Go}\right)}{\sigma_{\,Go}+2\sigma_{\,pf}+\widehat{\mathfrak{H}}_1\left(\sigma_{\,pf}-\sigma_{\,Go}\right)}$

Table 2. Influential characteristics of ternary nanofluids for the current designed model.

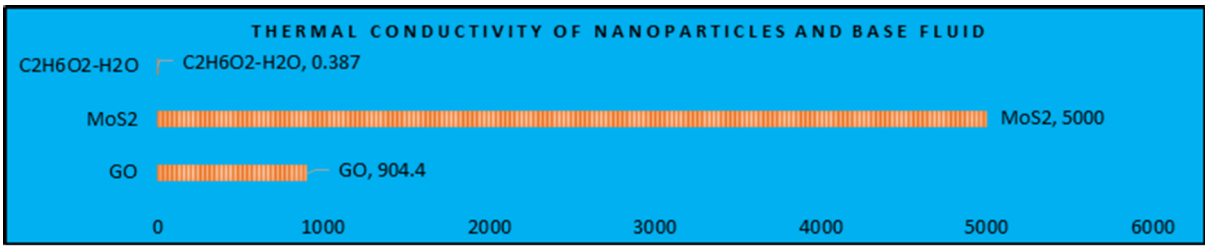

(a)

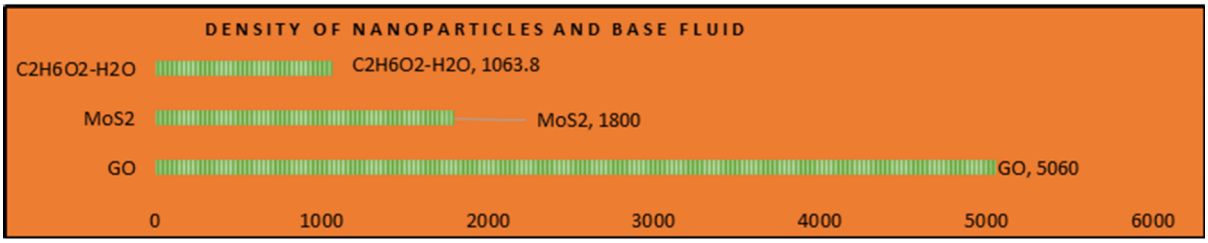

(b)

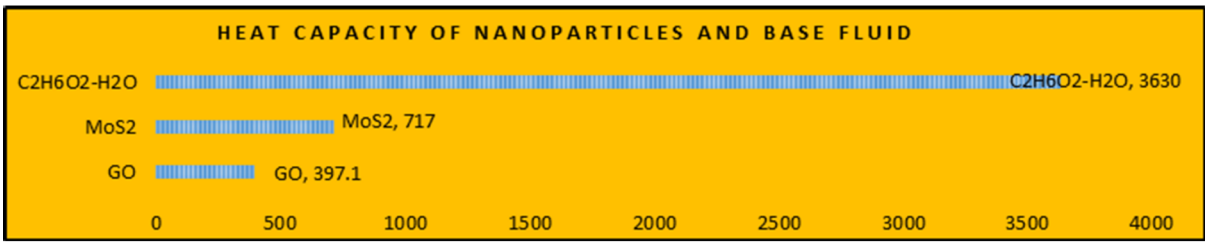

(c)

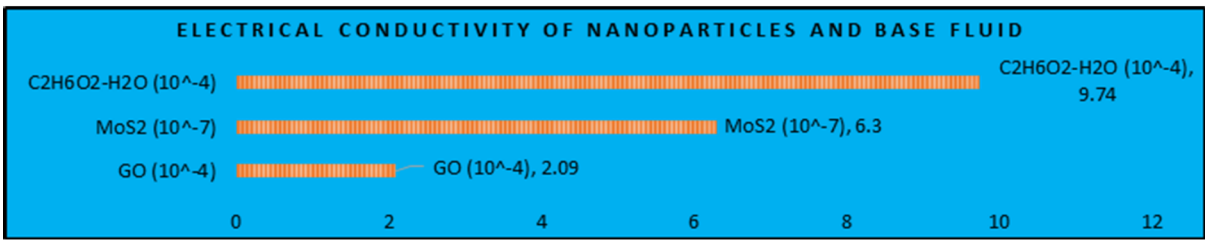

(d)

Fig. 2. The nanoparticles and hybrid base fluid properties.

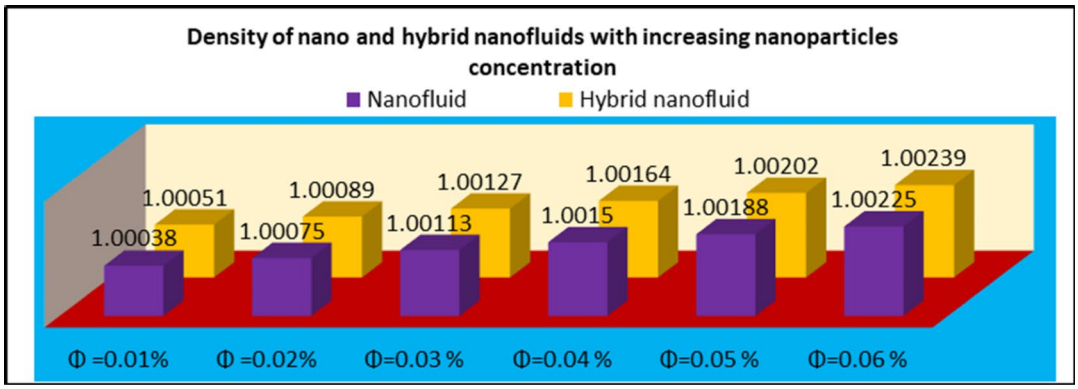

(a)

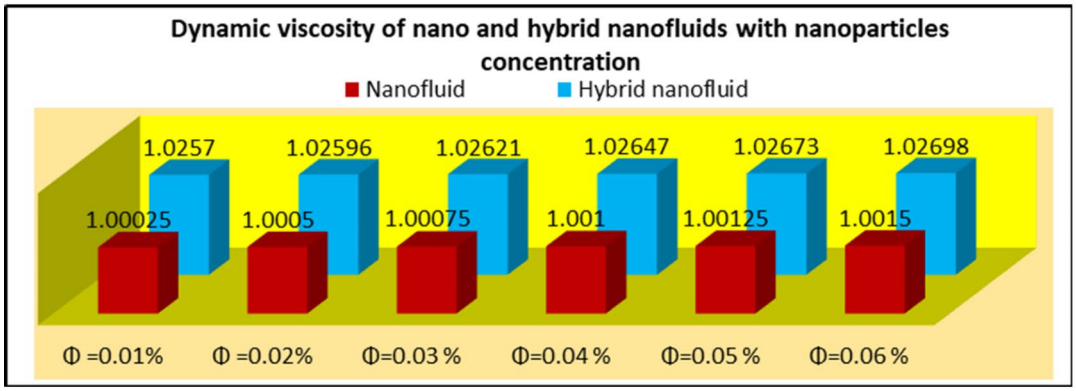

(b)

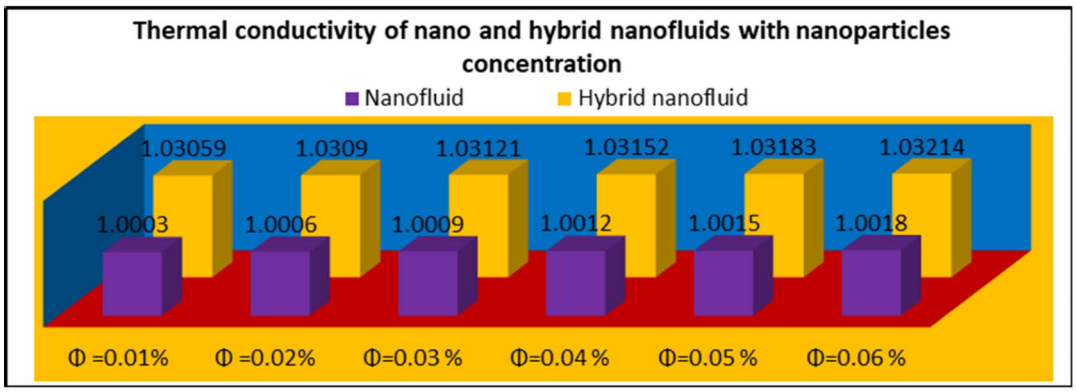

(c)

Fig. 3. The variations in nano and hybrid nanofluids with increasing nanoparticles amount.

The Eqs. (11–12) are obtained with appropriate differentiation and effective properties of nanofluids in Eqs. (6–7).

$$\left(\frac{2Re_x}{1+m}\right)^{1/2} C_{skinfric} = \frac{\mu_{\,hybridnano}}{\mu_{\,pf}} F\prime\prime\,(0) \tag{11}$$

$$\left(\frac{2}{(1+m)\,Re_x}\right)^{1/2} Nu = -\left(\frac{k_{hybridnano}}{k_{pf}} + Rd\right)\beta\,\prime\,(0) \tag{12}$$

The physical constraints embedded in the hybrid nanofluid model are wedge moving parameter ($\lambda = \frac{U_w}{U_\infty}$), Prandtl number ($Pr = \frac{\mu_{\,pf}(c_p)_{pf}}{k_{pf}}$), radiation number ($Rd = \frac{16\sigma^* T_\infty^3}{3k_{pf}k^*}$).

Mathematical analysis

Mathematical treatment of the model performed via numerical scheme usually termed as RK[40] scheme. After reducing the higher model problem into IVP[41], the propose scheme implemented successfully according to their standard procedure and executed the results for velocity and temperature fields for MRW (moving riga wedge) and SRW (static riga wedge) cases. The optimum values of η is considered 5 which represents the upper boundary limit. The numerical results for the velocity $F\prime\,(\eta)$ excellently fulfill the boundary conditions $F'(0) = \lambda = 0.3$ (MRW), $F'(0) = \lambda = 0.0$ (SRW), and upper boundary $F'(\infty) = F'(5) = 1.0$. Similarly, the temperature solutions for MRW and SRW showing good agreement with the boundary conditions. In both the cases, the temperature is examined as $\beta\,(0) = 1.0$ (at the surface) and asymptotic behaviour of the temperature starts beyond $\eta = 3.3$ which tells about the validity of the temperature condition $\beta\,(\infty) = 0$. These results are given in Table 3.

Stage I: At the first stage, the transformations associated to the problem are expressed as the following form.

$$\models_1 = F,\ \models_2 = F',\ \models_3 = F'',\ \models\prime_3 = F\prime\prime\prime \tag{13}$$

$$\models_4 = \beta,\ \models_5 = \beta',\ \models\prime_5 = \beta\prime\prime \tag{14}$$

Stage II: Arrange the obtained higher order problem into simplified form for both temperature and velocity.

$$F''' = \frac{\mu_{\,hybridnano}}{\mu_{\,pf}} \frac{\rho_{\,pf}}{\rho_{\,hybridnano}} \left[-FF'' - \frac{2m}{1+m}\left[1 - F'^2\right] - \frac{\sigma_{\,hybridnano}}{\sigma_{\,pf}} Me^{-\alpha\,\eta}\right] \tag{15}$$

$$\beta'' = -\left(\frac{k_{hybridnano}}{k_{pf}} + \frac{4}{3}Rd\right)^{-1} \left[\frac{Pr\,(\rho\,c_p)_{hybridnano}}{(\rho\,c_p)_{pf}}\left[F\beta' + Q\beta\right]\right] \tag{16}$$

Stage III: At this stage, the Eqs. (15–16) will transform in to the first order form using the associated functions from Eqs. (13–14).

$$\models\prime_3 = \frac{\mu_{\,hybridnano}}{\mu_{\,pf}} \frac{\rho_{\,pf}}{\rho_{\,hybridnano}} \left[-\models_1 \models_3 - \frac{2m}{1+m}\left[1 - \left(\models_2\right)^2\right] - \frac{\sigma_{\,hybridnano}}{\sigma_{\,pf}} Me^{-\alpha\,\eta}\right] \tag{17}$$

$$\models\prime_5 = -\left(\frac{k_{hybridnano}}{k_{pf}} + \frac{4}{3}Rd\right)^{-1} \left[\frac{Pr\,(\rho\,c_p)_{hybridnano}}{(\rho\,c_p)_{pf}}\left[\models_1 \models_5 + Q \models_4\right]\right] \tag{18}$$

Stage IV: The associated conditions and the transformed problem is then operated through coding in MATHEMATICA 13.0 and achieved the solutions and results due to varying parameters.

The present extended model is compared (Table 4) with the outcomes of Watanbe[42] under $Rd = 0$, $\varphi = 0$ and $\lambda = \frac{2m}{m+1}$. The output computed for skin friction and observed that the present results are well aligned with previous once and proves the reliability.

Results interpretation

A detailed investigation of the velocity, temperature, shear drag and Nusselt number for hybrid nanofluid under varying ranges of the physical parameters are demonstrated in this section. The results are interpreted for MRW and SRW cases for both the temperature and velocity fields.

Figure 4a-d presenting the velocity $F\prime$ of hybrid nanofluid for multiple ranges of λ, M, φ_1 and φ_2, respectively. The results reveal that the nanoliquid movement reduces for variable movement of the wedge (λ) and higher magnetic number values M. However, for accelerating RW, the particles movement is rapid than that of SRW. Physically, the fluid particles at the surface gain extra momentum due to the wedge movement which results increase in the velocity field. At the free stream, the fluid velocity is observed stable and no fluctuations are examined. This behaviour of the velocity represents that the imposed physical condition fulfilled. The next subset of Fig. 4c-d indicates the velocity variations when the nanoparticles amount augmented form 0.01 to 0.04. Higher dispersion of nanoparticles (GO-MoS_2) provided that the movement depreciates. Physically, high number of nanoparticles occupy space between the molecules and enhance the fluid's density. As a consequence

η	Velocity Solution		Temperature Solution	
	MRW Case $\lambda = 0.3$	SRW Case $\lambda = 0.0$	MRW Case $\lambda = 0.3$	SRW Case $\lambda = 0.0$
0.0	0.3	0.0	1.0	1.0
0.1	0.372447	0.089580	0.917856	0.936668
0.2	0.440879	0.174906	0.834197	0.871175
0.3	0.505235	0.255954	0.750049	0.803892
0.4	0.565462	0.332687	0.666559	0.735337
0.5	0.621525	0.405064	0.584946	0.666168
0.6	0.673406	0.473043	0.506436	0.597164
0.7	0.721116	0.536590	0.432192	0.529194
0.8	0.764689	0.595685	0.363238	0.463177
0.9	0.804194	0.650326	0.300403	0.400026
1.0	0.839730	0.700538	0.244270	0.340602
1.1	0.871428	0.746371	0.195146	0.285656
1.2	0.899446	0.787906	0.153061	0.235780
1.3	0.923975	0.825256	0.117789	0.191377
1.4	0.945224	0.858565	0.088882	0.152633
1.5	0.963425	0.888008	0.065730	0.119538
1.6	0.978823	0.913786	0.047615	0.091863
1.7	0.991670	0.936126	0.033772	0.069231
1.8	1.002220	0.955270	0.023444	0.051139
1.9	1.010730	0.971478	0.015923	0.037007
2.0	1.017450	0.985016	0.010578	0.026223
2.1	1.022610	0.996153	0.006871	0.018189
2.2	1.026440	1.005150	0.004364	0.012344
2.3	1.029130	1.012280	0.002709	0.008195
2.4	1.030870	1.017770	0.001643	0.005321
2.5	1.031830	1.021870	0.000744	0.003378
2.6	1.032150	1.024780	0.000564	0.002096
2.7	1.031970	1.026700	0.000319	0.001271
2.8	1.031380	1.027790	0.000176	0.000753
2.9	1.030480	1.028220	0.000095	0.000436
3.0	1.029350	1.028120	0.000050	0.000247
3.1	1.028040	1.027590	0.000025	0.000136
3.2	1.026620	1.026730	0.000012	0.000073
3.3	1.025100	1.025630	6.35×10^{-6}	0.000038
3.4	1.023540	1.024340	3.02×10^{-6}	0.000020
3.5	1.021940	1.022920	1.38×10^{-6}	0.000010
3.6	1.020340	1.021410	6.05×10^{-7}	5.02×10^{-6}
3.7	1.018740	1.019840	2.40×10^{-7}	2.44×10^{-6}
3.8	1.017140	1.018240	7.46×10^{-8}	1.18×10^{-6}
3.9	1.015570	1.016620	8.2×10^{-10}	5.74×10^{-7}
4.0	1.014020	1.015010	0	0
4.1	1.012490	1.013400	---	---
4.2	1.011000	1.011840	---	---
4.3	1.009530	1.010240	---	---
4.4	1.008090	1.008700	---	---
4.5	1.006670	1.007180	---	---
4.6	1.005290	1.005690	---	---
4.7	1.003939	1.004230	---	---
4.8	1.002590	1.002790	---	---
4.9	1.001280	1.001380	---	---
5.0	1.000000	1.000000	---	---

Table 3. Solutions of hybrid nanofluid model for the velocity and temperature for MRW and SRW cases.

m	Watanbe [42]	Current
0.0	0.46960	0.46954
0.0435	0.56898	0.56850
0.0909	0.65498	0.64872
0.20	0.80213	0.79513

Table 4. Validation of the problem results.

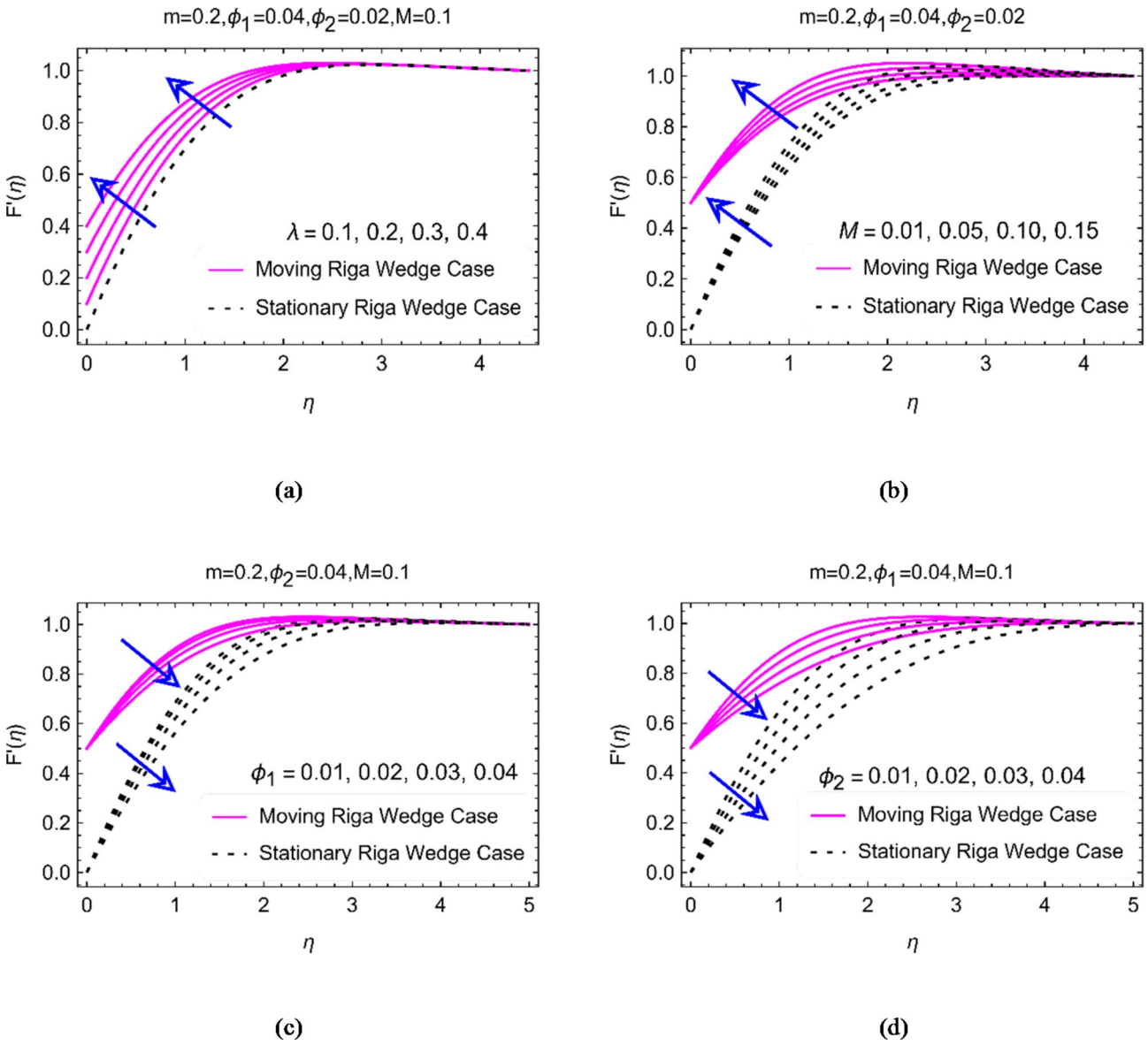

Fig. 4. The velocity distribution of hybrid nanofluid for (a) λ, (b) M, (c) φ_1 and (d) φ_2.

the intermolecular forces disturbed and bind the fluid particles tightly and the fluid motions drops. This means lessen the nanoparticles concentration lead to quite slow decrease in the movement.

The physical effects like heating source present in the fluid, solar thermal radiations, amount of nanoparticles, magnetic and moving surface aspects highly impact the temperature of hybrid nanofluids. Hence, the Fig. 5a-f designates to analyze the temperature performance of hybrid nanofluid under aforementioned physical phenomena. The heating source and solar radiations effectively enhanced the performance of (GO-MoS_2)/($C_2H_6O_2$-H_2O) in the range of 0.1,0.2,0.3,0.4 and 1.0,2.0,3.0,4.0, respectively. However, the fluid under stronger radiation effects is examined more efficient than heating source. Physically, the particles become more radiated due to externally applied thermal radiations which boosts the model performance. The surface layer

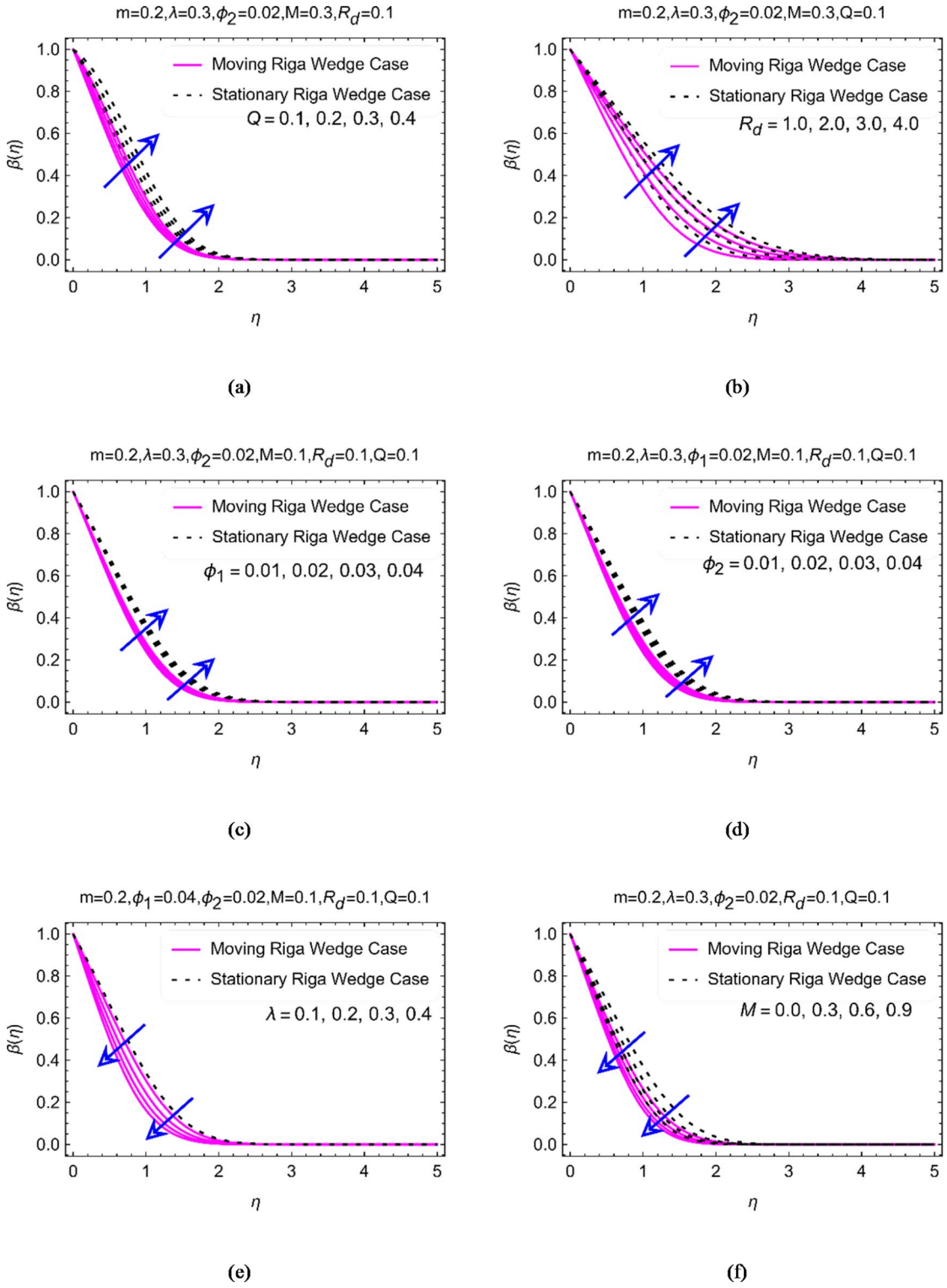

Fig. 5. The temperature distributions of hybrid nanoliquid for (a) Q, (b) Rd, (c) φ_1, (d) φ_2, (e) λ, and (f) M.

particles absorb heat and transfer it to the very next later which lead to augmentation in overall temperature performance. Further, the TBL over the surface is observed from $\eta = 0.0$ to $\eta \approx 2.0$ for heating source variations and $\eta = 0.0$ to $\eta \approx 3.5$ for radiations effects. This shows that for higher heating source number, the TBL reduced and the temperature asymptotically vanishes towards the ambient portion over the surface. The temperature approaches to 1 at $\eta = 0.0$.

Figure 5c-d and e-f highlighting the temperature performance for φ_1, φ_2, λ and M, respectively. It is observable that when the nanoparticles enhanced from 0.01 to 0.04, the temperature augmented. Physically, the thermal conductivity of the hybrid nanoliquid enhanced due to increasing number of nanoparticles and thermal conductivity of these particles. As a consequence, the whole thermal conductivity of the hybrid fluidic system enhanced due to which the temperature increase significantly. On the contrary, the moving parameter λ and magnetic number M controlled the temperature as mentioned in Fig. 5e-f. Hence, these two factors are observed excellent for the temperature reduction.

Figure 6a-b presenting the estimations for shear drag while Fig. 6c demonstrates the changes for heat transfer rate under augmented radiation number. It is obvious that the shear drag at the surface increases by strengthening the magnetic field effects. Physically, sophisticated magnetic field effects produces stronger Lorentz forces in the hybrid fluidic system which directly reduce the fluid movement. Due to this reason, the shear drag at the surface enhanced. Further, the skin friction declines for larger moving wedge number from 0.0 to 1.5. Physically, when the wedge movement increases the particles stuck at the surface get momentum and moves freely. This phenomena lead to drops in the shear drag for rapid RWG inside the fluid system. In the particular case, the heat transport rate reduces when radiation effects enhanced and these influences are demonstrated in Fig. 6c for simple, nano and hybrid nanofluidic systems.

The streamlines and isotherms variations for different default parametric values are furnished in Fig. 7a-h. The concentration of streamlines increases for stronger magnetic effects. When the strength of magnetic field increases, it shows resistance in the flow of nanofluid. Hence, the intensity of streamlines enhances towards the surface. Similarly, the heatlines are decorated for $Rd = 0.3$ and $Rd = 3.0$ with other default parameters values. The heatlines intensifies as the effects of radiation number changes from 0.3 to 3.0. Physically, the higher intensification of this phenomena is associated to the external energy provided by the radiations to the fluidic system. As a consequence, the heatlines increases.

Conclusions

The performance of hybrid nanomaterial (GO-MoS_2) suspended in hybrid base solvent ($C_2H_6O_2$-H_2O) is conducted in this research. The problem formulation was done via hybrid models for nanofluids and appropriate mathematical rules. The important physical aspects on the hybrid nanofluids for MRW and SRW are deeply discussed and concluded that:

- The hybrid functional liquid (GO-MoS_2)/($C_2H_6O_2$-H_2O) achieved optimum velocity for MRW case while it reaches to 1 towards free stream.
- The volume concentration of MoS_2 in the range of 0.01 to 0.04 highly resists the movement due to higher density and the intermolecular forces.
- The heat generating source and solar radiations number enhanced the performance of (GO-MoS_2)/($C_2H_6O_2$-H_2O) and better predicted ranges for these parameters are observed from $Q = 0.1,0.2,0.3,0.4$ and $Rd = 1.0,2.0,3.0,4.0$.
- The thin thermal boundary layer is examined for higher heat generating effects while it enlarges for the solar radiation effects.
- The increase in the amount of GO and MoS_2 nanoparticles from 0.01 to 0.04, result the thermal augmentation of (GO-MoS_2)/($C_2H_6O_2$-H_2O).
- The higher magnetic effects and MRW number λ controlled the thermal transport and thermal boundary layer.

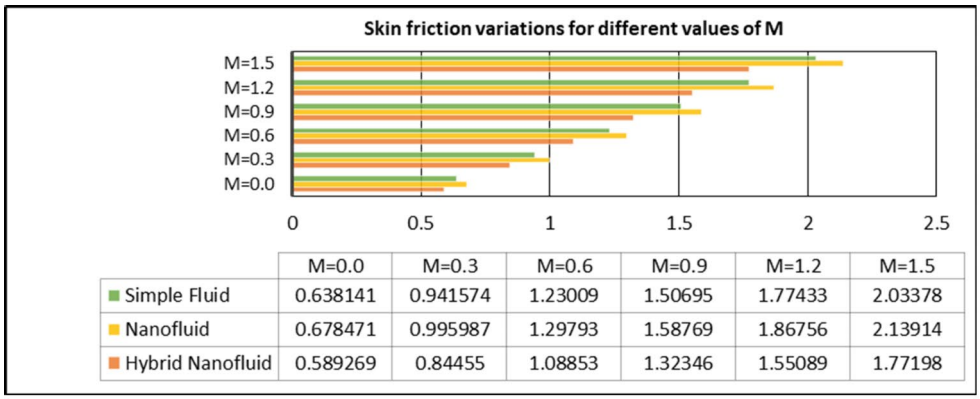

	M=0.0	M=0.3	M=0.6	M=0.9	M=1.2	M=1.5
Simple Fluid	0.638141	0.941574	1.23009	1.50695	1.77433	2.03378
Nanofluid	0.678471	0.995987	1.29793	1.58769	1.86756	2.13914
Hybrid Nanofluid	0.589269	0.84455	1.08853	1.32346	1.55089	1.77198

(a)

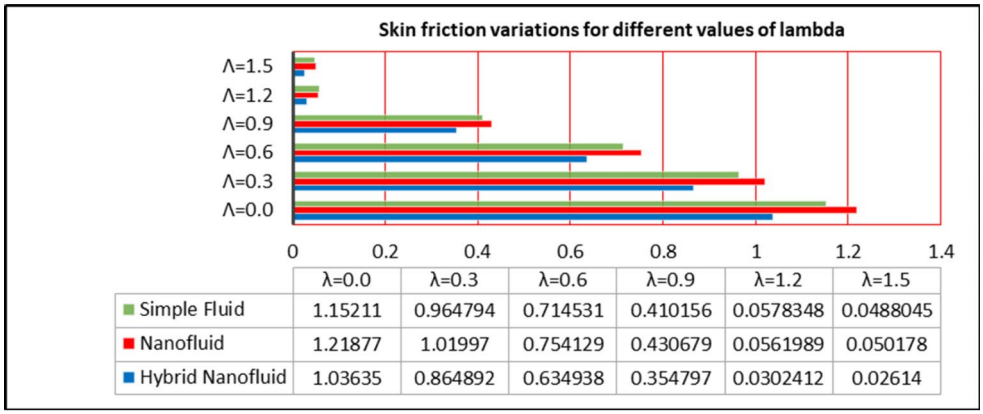

	λ=0.0	λ=0.3	λ=0.6	λ=0.9	λ=1.2	λ=1.5
Simple Fluid	1.15211	0.964794	0.714531	0.410156	0.0578348	0.0488045
Nanofluid	1.21877	1.01997	0.754129	0.430679	0.0561989	0.050178
Hybrid Nanofluid	1.03635	0.864892	0.634938	0.354797	0.0302412	0.02614

(b)

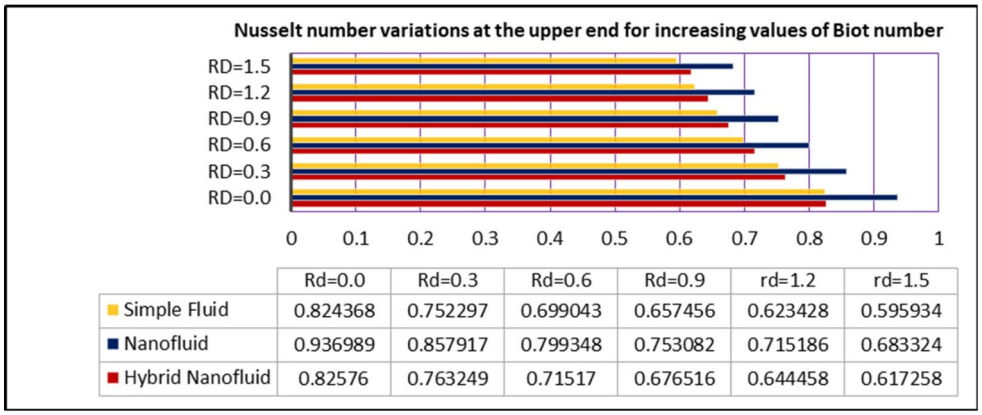

	Rd=0.0	Rd=0.3	Rd=0.6	Rd=0.9	rd=1.2	rd=1.5
Simple Fluid	0.824368	0.752297	0.699043	0.657456	0.623428	0.595934
Nanofluid	0.936989	0.857917	0.799348	0.753082	0.715186	0.683324
Hybrid Nanofluid	0.82576	0.763249	0.71517	0.676516	0.644458	0.617258

(c)

Fig. 6. The SF and Nu behaviour for higher parametric values.

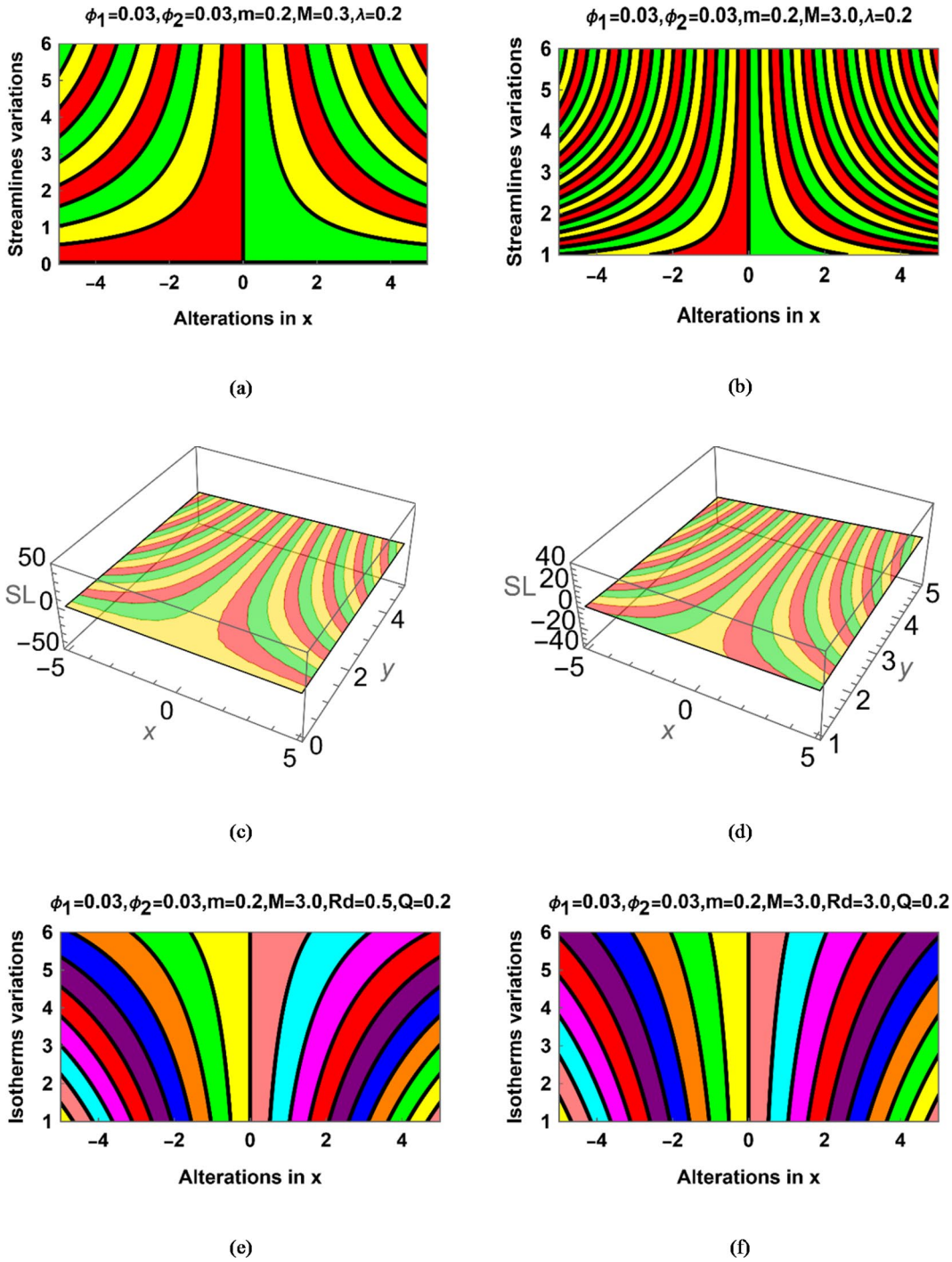

Fig. 7. The streamlines and heat lines trends for parametric values.

Data availability

The datasets used and/or analysed during the current study available from the corresponding author on reasonable request.

Received: 13 November 2024; Accepted: 10 January 2025
Published online: 31 January 2025

References

1. Madhukesh, J. K. et al. Numerical simulation of AA7072-AA7075/water-based hybrid nanofluid flow over a curved stretching sheet with Newtonian heating: A non-Fourier heat flux model approach. *J. Mol. Liq.* https://doi.org/10.1016/j.molliq.2021.116103 (2021).

2. Animasaun, I. L. et al. Insight into Darcy flow of ternary-hybrid nanofluid on horizontal surfaces: Exploration of the effects of convective and unsteady acceleration. *ZAMM J. Appl. Math. Mech.* https://doi.org/10.1002/zamm.202200197 (2022).
3. Saeed, A. et al. Three-dimensional casson nanofluid thin film flow over an inclined rotating disk with the impact of heat generation/consumption and thermal radiation. *Coatings* https://doi.org/10.3390/coatings9040248 (2019).
4. Mahanthesh, B., Mackolil, J. & Mallikarjunaiah, S. M. Response surface optimization of heat transfer rate in Falkner-Skan flow of ZnO − EG nanoliquid over a moving wedge: Sensitivity analysis. *Int. Commun. Heat Mass Transf.* https://doi.org/10.1016/j.icheatmasstransfer.2021.105348 (2021).
5. Adnan, S. et al. Thermal enhancement in Falkner-Skan flow of the nanofluid by considering molecular diameter and freezing temperature. *Sci. Rep.* https://doi.org/10.1038/s41598-022-13423-7 (2022).
6. Vahedi, S. M., Pordanjani, A. H., Raisi, A. & Chamkha, A. J. Sensitivity analysis and optimization of MHD forced convection of a Cu-water nanofluid flow past a wedge. *Eur. Phys. J. Plus* https://doi.org/10.1140/epjp/i2019-12537-x (2019).
7. Gowda, R. J. P., Kumar, R. N., Prasannakumara, B. C., Nagaraja, B. & Gireesha, B. J. Exploring magnetic dipole contribution on ferromagnetic nanofluid flow over a stretching sheet: An application of Stefan blowing. *J. Mol. Liquids* https://doi.org/10.1016/j.molliq.2021.116215 (2021).
8. Kumar, M. D. et al. Response surface methodology optimization of dynamical solutions of Lie group analysis for nonlinear radiated magnetized unsteady wedge: Machine learning approach (gradient descent). *Alex. Eng. J.* **74**, 29–50 (2023).
9. Sajjan, K. et al. Nonlinear Boussinesq and Rosseland approximations on 3D flow in an interruption of Ternary nanoparticles with various shapes of densities and conductivity properties. *AIMS Math.* **7**(10), 18416–18449 (2022).
10. Raju, C. S. K. et al. Nonlinear movements of axisymmetric ternary hybrid nanofluids in a thermally radiated expanding or contracting permeable Darcy Walls with different shapes and densities: Simple linear regression. *Int. Commun. Heat Mass Transf.* https://doi.org/10.1016/j.icheatmasstransfer.2022.106110 (2022).
11. Kumar, M. D., Raju, C. S. K., Sajjan, K., El-Zahar, E. R. & Shah, N. A. Linear and quadratic convection on 3D flow with transpiration and hybrid nanoparticles. *Int. Commun. Heat Mass Transf.* https://doi.org/10.1016/j.icheatmasstransfer.2022.105995 (2022).
12. Goud, B. S., Reddy, Y. D. & Adnan, A. Numerical investigation of the dynamics of magnetized casson nanofluid flow over a wedge subject to dissipation and thermal radiations. *Surf. Rev. Lett.* https://doi.org/10.1142/S0218625X24500549 (2024).
13. Mahmood, Z., Rafique, K., Khan, U., El-Rahman, M. A. & Alharbi, R. Analysis of mixed convective stagnation point flow of hybrid nanofluid over sheet with variable thermal conductivity and slip Conditions: A Model-Based study. *Int. J. Heat Fluid Flow* https://doi.org/10.1016/j.ijheatfluidflow.2024.109296 (2024).
14. Alghamdi, W. et al. Boundary layer stagnation point flow of the Casson hybrid nanofluid over an unsteady stretching surface. *AIP Adv.* https://doi.org/10.1063/5.0036232 (2021).
15. Bani-Fwaz, M. Z. et al. Investigation of unsteady nanofluid over half infinite domain under the action of parametric effects and EPNM. *J. Therm. Anal. Calorim.* https://doi.org/10.1007/s10973-024-13121-8 (2024).
16. Khadija, R. et al. Numerical investigation of entropy generation of Joule heating in non-axisymmetric flow of hybrid nanofluid towards stretching surface. *J. Comput. Des. Eng.* **11**(2), 146–160 (2024).
17. Adnan, A., Nadeem, A. & Said, N. M. LSM analysis of thermal enhancement in KKL model-based unsteady nanofluid problem using CCM and slanted magnetic field effects. *J. Therm. Anal. Calorim.* **149**, 839–851 (2024).
18. Reddy, M. G., Gowda, R. J. P., Kumar, R. V., Prasannakumara, B. C. & Kumar, K. G. Analysis of modified Fourier law and melting heat transfer in a flow involving carbon nanotubes. *Part E J. Process Mech. Eng.* https://doi.org/10.1177/09544089211001353 (2021).
19. Gul, H., Ramzan, M., Saleel, C. A., Kadry, S. & Saeed, A. M. "Heat transfer analysis of a moving wedge with impact of nano-layer on nanofluid flows comprising magnetized carbon nanomaterials. *Numer. Heat Transf. Part A Appl.* https://doi.org/10.1080/10407782.2023.2240498 (2023).
20. Waseem, A., Eladeb, A. & Kolsi, L. Numerical analysis of thermal improvement in hydrogen-based host fluids under buoyancy force and EPNM effects: Study for vertical cylinder. *ZAMM J. Appl. Math. Mech.* https://doi.org/10.1002/zamm.202200449 (2024).
21. Punith, R. J. G., Kumar, R. N., Madhukesh, J. K., Prasannakumara, B. C. & Gorla, R. S. R. Theoretical analysis of SWCNT-MWCNT/H2O hybrid flow over an upward/downward moving rotating disk. *Part N J. Nanomater. Nanoeng. Nanosyst.* https://doi.org/10.1177/2397791420980282 (2021).
22. Reddy, C. A., Thumma, T., Goud, J. S. & Panda, S. Thermal and sensitivity analysis on hydromagnetic CuO-Ag-H2O nanofluid radiative flow over an elongating convective thermal surface: RSM-CCD model. *J. Therm. Anal. Calorim.* **148**, 12195–12210 (2023).
23. Shamshuddin, M. D. et al. Thermal case exploration of electromagnetic radiative tri-hybrid nanofluid flow in Bi-directional stretching device in absorbent medium: SQLM analysis. *Case Stud. Therm. Eng.* https://doi.org/10.1016/j.csite.2024.104734 (2024).
24. Shamshuddin, M. D., Panda, S., Pattnaik, P. K. & Mishra, S. R. Ferromagnetic and ohmic effects on nanofluid flow via permeability rotative disk: Significant interparticle radial and nanoparticle radius. *Phys. Script.* https://doi.org/10.1088/1402-4896/ad35f8 (2024).
25. Shamshuddin, M. D., Panda, S., Saeed, A., Ratha, P. K. & Mishra, S. R. Homotopy analysis on magnetized Williamson-micropolar nanofluid flow over a bi-directionally extending surface with multiple slip conditions. *Numer. Heat Transf. Part B: Fundam.* https://doi.org/10.1080/10407790.2024.2364783 (2024).
26. Waqas, H. et al. Heat transfer analysis of hybrid nanofluid flow with thermal radiation through a stretching sheet: A comparative study. *Int. Commun. Heat Mass Transf.* https://doi.org/10.1016/j.icheatmasstransfer.2022.106303 (2022).
27. Ferdows, M., Shamshuddin, M., Rashad, A. M., Murtaza, M. G. & Salawu, S. O. Three-dimensional boundary layer flow and heat/mass transfer through stagnation point flow of hybrid nanofluid. *J. Eng. Appl. Sci.* https://doi.org/10.1186/s44147-024-00388-9 (2024).
28. Adnan, A. & Ashraf, W. Analysis of heat transfer performance for ternary nanofluid flow in radiated channel under different physical parameters using GFEM. *J. Taiwan Inst. Chem. Eng.* https://doi.org/10.1016/j.jtice.2023.104887 (2023).
29. Alqahtani, A. M., Khan, U., Ahmed, N., Mohyud-Din, S. T. & Khan, I. Numerical investigation of heat and mass transport in the flow over a magnetized wedge by incorporating the effects of cross-diffusion gradients: Applications in multiple engineering systems. *Math. Probl. Eng.* https://doi.org/10.1155/2020/2475831 (2020).
30. Kudenatti, R. B. & Jyothi, B. Two-dimensional boundary-layer flow and heat transfer over a wedge: Numerical and asymptotic solutions. *Therm. Sci. Eng. Progr.* **11**, 66–73 (2019).
31. Amar, N., Kishan, N. & Goud, B. S. MHD heat transfer flow over a moving wedge with convective boundary conditions with the influence of viscous dissipation and internal heat generation/absorption. *Heat Transfer* https://doi.org/10.1002/htj.22534 (2022).
32. Anuar, N. S., Bachok, N., Arifin, N. M. & Rosali, H. Analysis of Al2O3-Cu nanofluid flow behaviour over a permeable moving wedge with convective surface boundary conditions. *J. King Saud Univ. Sci.* https://doi.org/10.1016/j.jksus.2021.101370 (2021).
33. Zeeshan, A., Hussain, D., Asghar, Z., Bhatti, M. M. & Duraihem, F. Z. Thermal optimization of MHD nanofluid over a wedge by using response surface methodology: Sensitivity analysis. *Propuls. Power Res.* **12**(4), 556–567 (2023).
34. Khan, U., Ahmed, N. & Mohyud-Din, S. T. Heat transfer enhancement in hydromagnetic dissipative flow past a moving wedge suspended by H2O-aluminum alloy nanoparticles in the presence of thermal radiation. *Int. J. Hydrogen Energy* **42**(39), 24634–24644 (2017).
35. Raju, S. S. K. et al. Contour analysis for heat transfer rate in a wedge geometry with non-uniform shapes nanofluid: Gradient descent machine learning technique. *Results Eng.* https://doi.org/10.1016/j.rineng.2024.102714 (2024).

36. Adnan, A. & Ashraf, W. Thermal efficiency in hybrid (Al2O3-CuO/H2O) and ternary hybrid nanofluids (Al2O3-CuO-Cu/H2O) by considering the novel effects of imposed magnetic field and convective heat condition. *Waves in Random and Complex Media* https://doi.org/10.1080/17455030.2022.2092233 (2022).
37. Alharbi, K. A. M., Nadeem, A. & Eldin, S. M. Heat transport mechanism in glycerin-titania nanofluid over a permeable slanted surface by considering nanoparticles aggregation and Cattaneo Christov thermal flux. *Sci. Progr.* https://doi.org/10.1177/00368504231180032 (2023).
38. Mishra, N. K. et al. Investigation of improved heat transport featuring in dissipative ternary nanofluid over a stretched wavy cylinder under thermal slip. *Case Stud. Therm. Eng.* https://doi.org/10.1016/j.csite.2023.103130 (2023).
39. Waseem, A., Eldin, S. M. & Bani-Fwaz, M. Z. Numerical investigation of non-transient comparative heat transport mechanism in ternary nanofluid under various physical constraints. *AIMS Math.* **8**(7), 15932–15949 (2023).
40. Khalid, A. M. A. & Adnan,. Thermal investigation and physiochemical interaction of H2O and C2H6O2 saturated by Al2O3 and γAl2O3 nanomaterials. *J. Appl. Biomater. Funct. Mater.* https://doi.org/10.1177/22808000221136483 (2022).
41. AL-Zahrani, A. A., Mahmood, I., Khaleeq, U. R., Tag-Eldin, E. & Bani-Fwaz, M. Z. Analytical study of (Ag–Graphene)/blood hybrid nanofluid influenced by (platelets-cylindrical)nanoparticles and Joule heating via VIM. *ACS Omega* **8**(22), 19926–19938 (2023).
42. Watanabe, T. Thermal boundary layers over a wedge with uniform suction or injection in forced flow. *Acta Mech.* **83**, 119–126 (1990).

Acknowledgements

The authors extend their appreciation to the Deanship of Research and Graduate Studies at King Khalid University for funding this work through Large Research Project under grant number RGP2/78/45.

Author contributions

M.Z.B.F and Adnan: Conceptualization, Model formulation, Software, writing original draft, validationS.U.K., B.S.G., T.W., K.K.A. and I.T.: Conceptualization, Formal analysis, methodology, software, validation. Adnan and S.U.K.: Writing review and editing.

Declarations

Competing interests

The authors declare no competing interests.

Additional information

Supplementary Information The online version contains supplementary material available at https://doi.org/10.1038/s41598-025-86470-5.

Correspondence and requests for materials should be addressed to T.W.

Reprints and permissions information is available at www.nature.com/reprints.

Publisher's note Springer Nature remains neutral with regard to jurisdictional claims in published maps and institutional affiliations.